Chaos

Control of escapes in two-degree-of-freedom open Hamiltonian systems

Cite as: Chaos **32**, 063118 (2022); https://doi.org/10.1063/5.0090150
Submitted: 03 March 2022 • Accepted: 16 May 2022 • Published Online: 10 June 2022

Alexandre R. Nieto, Thomas Lilienkamp, Jesús M. Seoane, et al.

Control of escapes in two-degree-of-freedom open Hamiltonian systems

Cite as: Chaos **32**, 063118 (2022); doi: 10.1063/5.0090150
Submitted: 3 March 2022 · Accepted: 16 May 2022 ·
Published Online: 10 June 2022

Alexandre R. Nieto,[1] Thomas Lilienkamp,[2] Jesús M. Seoane,[1] Miguel A. F. Sanjuán,[1,3] and Ulrich Parlitz[2,4,a)]

AFFILIATIONS

[1]Nonlinear Dynamics, Chaos and Complex Systems Group, Departamento de Física, Universidad Rey Juan Carlos, Tulipán s/n, 28933 Móstoles, Madrid, Spain
[2]Max Planck Institute for Dynamics and Self-Organization, Am Fassberg 17, 37077 Göttingen, Germany
[3]Department of Applied Informatics, Kaunas University of Technology, Studentu 50-415, Kaunas LT-51368, Lithuania
[4]Institute for the Dynamics of Complex Systems, University of Göttingen, Friedrich-Hund-Platz 1, 37077 Göttingen, Germany

[a)]**Author to whom correspondence should be addressed:** ulrich.parlitz@ds.mpg.de

ABSTRACT

We investigate the possibility of avoiding the escape of chaotic scattering trajectories in two-degree-of-freedom Hamiltonian systems. We develop a continuous control technique based on the introduction of coupling forces between the chaotic trajectories and some periodic orbits of the system. The main results are shown through numerical simulations, which confirm that all trajectories starting near the stable manifold of the chaotic saddle can be controlled. We also show that it is possible to *jump* between different unstable periodic orbits until reaching a stable periodic orbit belonging to a Kolmogorov–Arnold–Moser island.

Control of chaos in Hamiltonian systems is a relevant topic in physics that has aroused much attention in recent decades. However, mainly, discrete control schemes have been implemented. In this manuscript, we show that a continuous control inspired by the Pyragas method can be used to avoid the escape of trajectories in two-degree-of-freedom Hamiltonian systems, which are quite common in chaotic scattering problems. The control scheme starts with a systematic search of symmetric periodic orbits (SPOs) and their crossings with a predefined control axis. Once an arbitrary trajectory crosses this axis, a coupling force between the trajectory and a symmetric periodic orbit is activated. In the presence of the control force, the trajectory approaches the desired periodic orbit, thereby avoiding the escape. After some time, the control force becomes almost negligible and the system recovers its original energy. We test the effectiveness of the method by applying the control to a huge number of initial conditions, distributed along representative Poincaré sections. The numerical simulations show that a significant percentage of escaping initial conditions can be kept within the scattering region by using weak coupling forces and a relatively small amount of symmetric periodic orbits. The initial conditions that are not possible to control are those located far from the stable manifold of the chaotic saddle. In the final part of the work, we show that once a trajectory is stabilized into some periodic orbit, it is possible to move it to different periodic orbits by changing the coupling force at an appropriate time. The goal of this extension of the method is not only to avoid the escape but also to choose in which particular periodic orbit we want to stabilize the system. We hope this work will be useful in research fields such as fusion plasmas, celestial mechanics, conservative flows, and laser-driven reactions.

I. INTRODUCTION

Chaotic scattering is an important topic in nonlinear science and it has numerous applications in classical[1] and quantum physics.[2] Many chaotic scattering processes occur in open Hamiltonian systems, which are conservative systems characterized by a potential through which trajectories can escape toward infinity. Therefore, in a standard chaotic scattering problem, trajectories exhibit a transient chaotic motion inside a scattering region. Many works on the subject

have studied the main characteristics of the escape dynamics and the associated ubiquitous fractal structures.[3,4] However, another important task is to prevent the escape of trajectories by using control techniques.

After the pioneering work of Ott, Grebogi, and Yorke (OGY),[5] the field of controlling chaos blossomed and many experimental, theoretical, and numerical results have been obtained since then. In addition to dissipative systems, much work has been done in the context of conservative chaos. In particular, some early works extended the OGY method to Hamiltonian chaos.[6,7] Also, different existing techniques like the partial control method[8] have been applied to conservative systems. Nevertheless, specific methods have also been developed.[9,10] Some examples of applications include the control of periodically driven Hamiltonian systems,[11] control of anomalous transport in plasmas,[12] and control of conservative flows in the presence of noise.[13] Despite the wide variety of research, continuous control techniques have not received much attention.

The main goal of this paper is to provide a continuous control method to avoid the escapes of trajectories in open Hamiltonian systems. In particular, we have chosen as a model the paradigmatic Hénon–Heiles Hamiltonian,[14] which is a two-degree-of-freedom dynamical system. For our purposes, we have implemented a continuous control method without feedback, inspired by the Pyragas control method for dissipative systems.[15]

The basic idea of the method is to avoid the escape of trajectories by including a coupling force between the chaotic escaping trajectory and a periodic orbit. For that purpose, first we need to establish in which periodic orbit of the system we want to stabilize the trajectory. Since most open Hamiltonian systems exhibit several symmetries, their periodic orbits are also symmetric and can be easily obtained. Our results show that by considering only a few symmetric periodic orbits (SPOs), it is possible to keep most trajectories within the scattering region. In particular, all the trajectories starting from initial conditions close to the stable manifold of the chaotic saddle can be controlled.

Moreover, we also show that once the original escaping trajectory has been stabilized into a controlled periodic orbit, it is possible to jump between different SPOs until achieving a desired and predefined periodic orbit. We illustrate this idea to show the stabilization of the system in a periodic orbit located in the center of a Kolmogorov–Arnold–Moser (KAM) torus. Since this orbit is stable, we can turn off the coupling force here once the desired orbit is reached. For low energy levels, most Hamiltonian systems exhibit KAM islands embedded within the chaotic saddle, so to reach one of them is a natural control strategy.

The organization of this manuscript is as follows. First, in Sec. II, we describe the model of study. In Sec. III, a brief explanation about the method for computing SPOs is offered. The control scheme and some particular examples of its implementation are shown in Sec. IV. A general analysis of the effectiveness of the method, based on extensive numerical simulations for many different initial conditions, is carried out in Sec. V. The extension of the control method, showing the possibility of moving between different SPOs, is explained in Sec. VI. Finally, in Sec. VII, we present the main conclusions of this manuscript.

II. MODEL DESCRIPTION

The Hénon–Heiles system is a paradigmatic 2D time independent Hamiltonian system in nonlinear dynamics, and this explains why is so widely studied. It owes its name to the French astronomer Michel Hénon and the American astrophysicist Carl Heiles, who in 1964 used it in their search for the third integral of motion. The Hamiltonian is given by

$$\mathcal{H} = \frac{1}{2}(\dot{x}^2 + \dot{y}^2) + \frac{1}{2}(x^2 + y^2) + x^2 y - \frac{1}{3}y^3. \tag{1}$$

As a consequence, the equations of motion read

$$\begin{aligned} \dot{x} &= p_x, \\ \dot{y} &= p_y, \\ \dot{p_x} &= -x - 2xy, \\ \dot{p_y} &= -y - x^2 + y^2. \end{aligned} \tag{2}$$

To visualize the system, we represent the isopotential curves for different values of the energy in Fig. 1. When the energy is below the threshold $E_e < 1/6$, known as the escape energy, the isopotential curves are closed. However, when its value is above the escape energy, three symmetrical exits separated by an angle $2\pi/3$ radians appear. This is a consequence of the presence of three saddle points in the potential well, which are represented with red dots in the figure. Therefore, it is for $E > E_e$ when the system becomes a paradigmatic example of chaotic scattering.

There are trajectories that do not escape from the scattering region for energy values slightly above the escape energy. Most of these trajectories describe periodic or quasiperiodic motion inside a KAM torus. Nonetheless, as a consequence of the destruction of resonant islands and the subsequent formation of cantori, there are also non-escaping chaotic trajectories inside the KAM islands. In this work, we have applied the control method to the system with energy

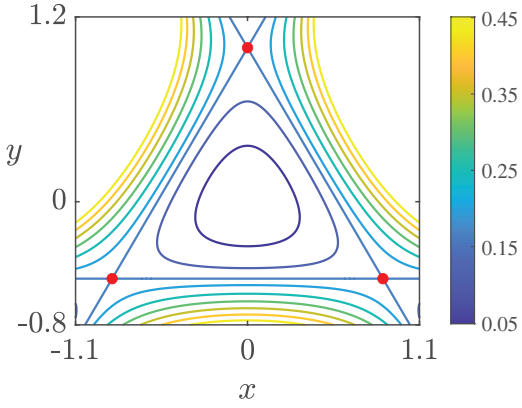

FIG. 1. Isopotential curves of the Hénon–Heiles system for different values of the potential $V(x, y) = \frac{1}{2}(x^2 + y^2) + x^2 y - \frac{1}{3}y^3$. The color of the curves indicates the value of the potential, according to the color bar. Values below and above the escape energy $E_e = 1/6$ are represented. The red dotes are located in the three saddle points of the potential.

$E = 0.2$, for which only one small region of KAM orbits exists, occupying a negligible fraction of the phase space. Inside and around this KAM island, there may be small resonant islands of higher order that we have not considered as a target in the control scheme.

III. SEARCH OF SYMMETRIC PERIODIC ORBITS

The basic idea of the continuous control method that we have implemented is to avoid the escape of trajectories by stabilizing a periodic orbit of the system. Our aim is not to show that a particular trajectory can be kept in the scattering region but to construct a set of periodic orbits that allows us to avoid the escaping of a high percentage of arbitrary initial conditions. Hence, the first step is to obtain the location of some periodic orbits of the system.

As long as we are facing a Hamiltonian system, there are no chaotic attractors in the phase space. However, a skeleton of symmetric periodic orbits is embedded within the chaotic saddle. The stable directions of these periodic orbits make up the stable manifold of the chaotic saddle. To locate and compute the skeleton of periodic orbits in a Hamiltonian system is an old and challenging problem, for which many different techniques have been developed (see, for example, Refs. 16 and 17). In this research, we have located and computed SPOs following the accurate method described in Ref. 18, which for completeness we will briefly summarize here.

The Hénon–Heiles system is time-reversible and has a D_3 symmetry (this is the symmetry group of an equilateral triangle). As a consequence, the periodic orbits are symmetric about the y axis and two other axes. Bearing this in mind, SPOs can be found by looking for perpendicular intersections with any of these symmetry axis. For convenience, we find the periodic orbits that are symmetric about the y axis. Therefore, we can say that if a trajectory starts at $x = 0$ being perpendicular to the y axis (hence, $\dot{y}_0 = 0$ and $\dot{x}_0$ is fixed by the energy such that $\dot{x}_0 = \sqrt{2E - y_0^2 + 2y_0^3/3}$), and eventually crosses that axis again perpendicularly, then this trajectory is an SPO. The number of crossings between perpendicular intersections is the multiplicity m of the SPO. On the other hand, the double the time needed to return perpendicularly to the y-axis is the period T of the SPO. Therefore, the condition for an SPO is $x(0, y_0, \dot{x}_0, 0; T/2) = \dot{y}(0, y_0, \dot{x}_0, 0; T/2) = 0$.

From a computational point of view, we proceed to launching initial conditions $(0, y_0, \dot{x}_0, 0)$ for many values of y_0 (we recall that $\dot{x}_0$ is perfectly fixed by the energy). For every initial condition, we calculate the coordinates after m crossings with the y axis. If for two consecutive values of y_0 the sign of $\dot{y}$ in the mth crossing changes, it means that between these two values there is an SPO. For a simple realization of the method, we will observe as many changes in the sign as SPOs can be detected with the precision of the numerical simulation. In particular, the smaller the step between values of y_0, the higher will be the number of SPOs that we can detect.

Once a change in sign is detected, we proceed with a bisection method that returns with high accuracy the coordinate y_s where the SPO crosses perpendicularly the y axis. In our case, we have located the SPOs with a double precision of up to 16 significant decimal digits. Once the coordinate y_s is known, we just have to compute the orbit during one period in order to know its coordinates at any time. We repeat this procedure for every change in sign obtained.

It is worthwhile to mention that the method not only detects the SPOs of a given multiplicity m but also the SPOs of multiplicities that are integer divisors of m. For example, a unique numerical simulation brings the SPOs of multiplicities 10, 5, 2, and 1.

To illustrate this method and the SPOs themselves, we show some examples of SPOs of different multiplicities in Fig. 2. The blue curves represent the SPOs, while the dots located in the y axis refer to the perpendicular intersections of the SPOs. These points are exactly the ones that are detected by the search algorithm. The red dots indicate that the SPO is unstable, while the green dots indicate the opposite.

Four different SPOs are depicted in Fig. 2(a), all of them of multiplicity 1. Three of these orbits, labeled $\Pi_{4,7,8}$ following the notation of Churchill,[19] are called nonlinear normal modes (NNMs). They have received special interest as their existence is a direct consequence of the symmetries of the system. $\Pi_{7,8}$ follow the same path but in the opposite direction, as a consequence of the time-reversal symmetry. $\Pi_{4,5,6}$ (here only Π_4 is represented) are a consequence of the D_3 symmetry. Finally, $\Pi_{1,2,3}$ only exist when the system is closed ($E < 1/6$) and, therefore, cannot be represented here. The last SPO appearing in Fig. 2(a), labeled as L_1, is one of the three Lyapunov orbits.[20] We recall that when any trajectory crosses a Lyapunov orbit with its velocity vector pointing outward of the exit, it will escape to infinity and will never come back. These orbits are located in the vicinity of the exits, passing through the saddle points of the potential. In Sec. VI, we will show that the Lyapunov orbit L_1, due to its singular location close to the exits, is the only SPO that is not possible to use to stabilize the trajectories of the system.

On the other hand, in panels (b), (c), and (d) of Fig. 2, we represent three SPOs of multiplicity 2, 4, and 8, respectively. The SPO of multiplicity 2 is special since it is the main stable symmetric periodic orbit of the system, and it corresponds to the center of a KAM island. In Sec. VI, we will show that, if desired, it is possible to use the control scheme to move any stabilized SPO into this singular periodic orbit.

Since the system is open, the stable or unstable character of a periodic orbit can be elucidated on the basis of whether trajectories starting from initial conditions that are infinitesimally close to a periodic orbit escape or not. In this sense, trajectories starting from initial conditions close to a stable periodic orbit will remain close forever and, therefore, will not escape. On the contrary, initial conditions close to an unstable periodic orbit will eventually leave the chaotic saddle and escape to infinity. The reason is that the unstable periodic orbits form a set of Lebesgue measure zero. Therefore, an infinite precision is required in order to find an initial condition that belongs to an unstable periodic orbit. Put another way, the probability that randomly chosen initial conditions belong to an unstable periodic orbit is zero. This simple criterion is not valid in the case of unstable periodic orbits trapped inside a KAM island. In these situations, different methods could be used to determine the stability.[21,22] Nevertheless, in this work, we have considered unstable periodic orbits located in the chaotic sea, so the criterion based on the escape is appropriate.

For the implementation of the control scheme, we have computed a total of 200 SPOs of multiplicities 8, 4, 2, and 1. The only reason to select this number of SPOs is to show that it is possible to avoid the escape of the trajectories by using a relatively small number

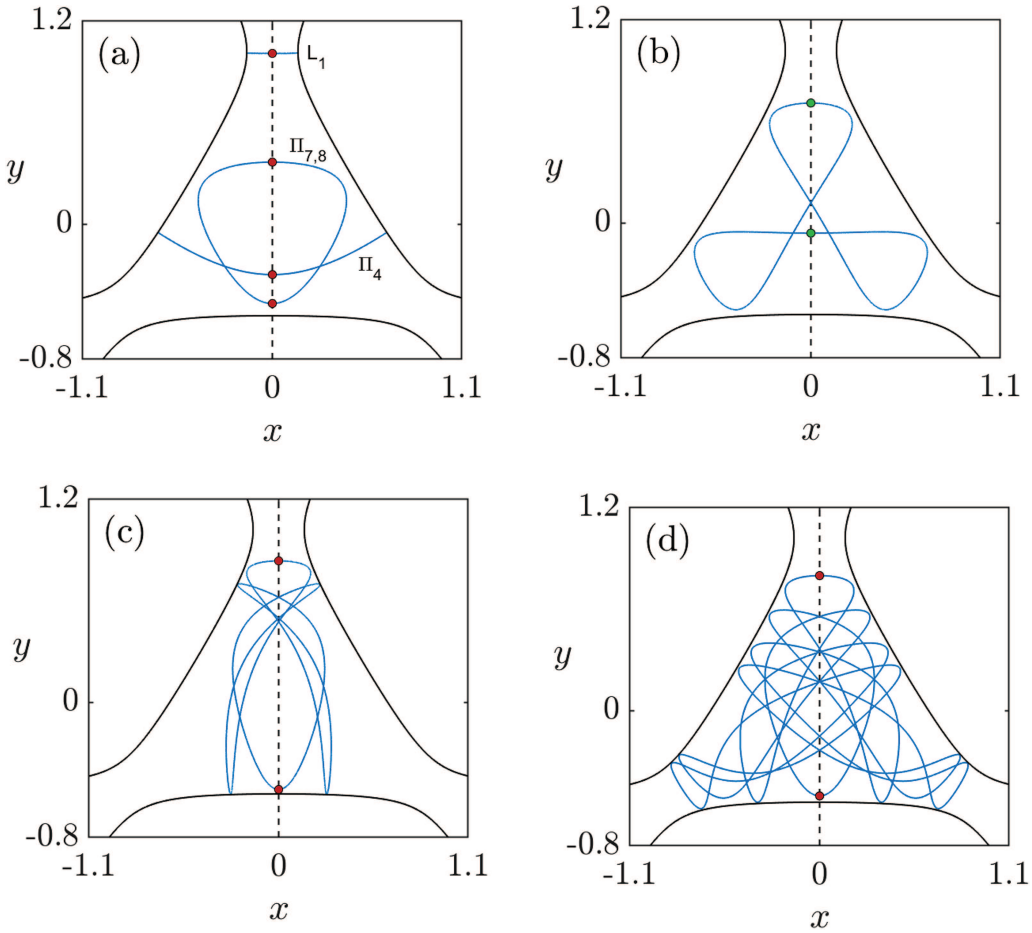

FIG. 2. Projections in the physical space of SPOs of multiplicity (a) 1, (b) 2, (c) 4, and (d) 8. All these periodic orbits are symmetric about the y axis, which is highlighted with a dark dashed line. The red and green dots along the y axis are located in perpendicular crossings of the SPOs with that axis. The color red (green) of the dots indicates that the SPO is unstable (stable). From the SPOs represented in panel (a), three are nonlinear normal modes ($\Pi_{4,7,8}$) and one is a Lyapunov orbit (L_1).

of SPOs. However, to compute a higher number is computationally effortless, so the total amount of orbits that are used to control the escape will depend basically on the needs of the particular problem. In our case, for calculating the SPOs, we have made a single numerical simulation in which we have launched 5×10^4 equally spaced initial conditions along the segment $y \in [-0.542, 1.2]$.

These 200 SPOs cross the y axis a total of 2460 times. All these crossings define the set of points that we will use to start the control of the trajectories. For each individual trajectory, the choice of the target SPO will be based on the Euclidean metric in the $y - \dot{y}$ plane between the trajectory and the crossings.

IV. IMPLEMENTATION OF THE CONTROL SCHEME

In Sec. III, we have explained the method that we have used to compute the SPOs of the system. Once these orbits have been obtained, we can use them in our control scheme to avoid the escape of the trajectories.

Now, we consider that a random initial condition has been launched. Without control, the trajectory will escape after describing a chaotic transient. Our aim is to introduce a coupling between the trajectory and an SPO, achieving a controlled periodic behavior instead of a transient chaotic motion. The control of the trajectory will start at the moment in which it crosses the y axis. However, which SPO should we use for the coupling? For taking this decision, we calculate the Euclidean metric between the crossing point and all the crossings of the SPOs that we have previously calculated. From all of them, we choose the one that minimizes the Euclidean metric, namely,

$$\min\{d_i\} = \min\left\{\sqrt{(y_c - y_{s,i})^2 + (|\dot{y}_c| - |\dot{y}_{s,i}|)^2}\right\}, \qquad (3)$$

with $y_c, \dot{y}_c$ being the coordinates of the trajectory in $x = 0$ and $y_{s,i}, \dot{y}_{s,i}$ the coordinates of the ith crossing of our 200 SPOs (we recall that here $i = 1, 2, \ldots, 2460$). We have taken absolute values in the

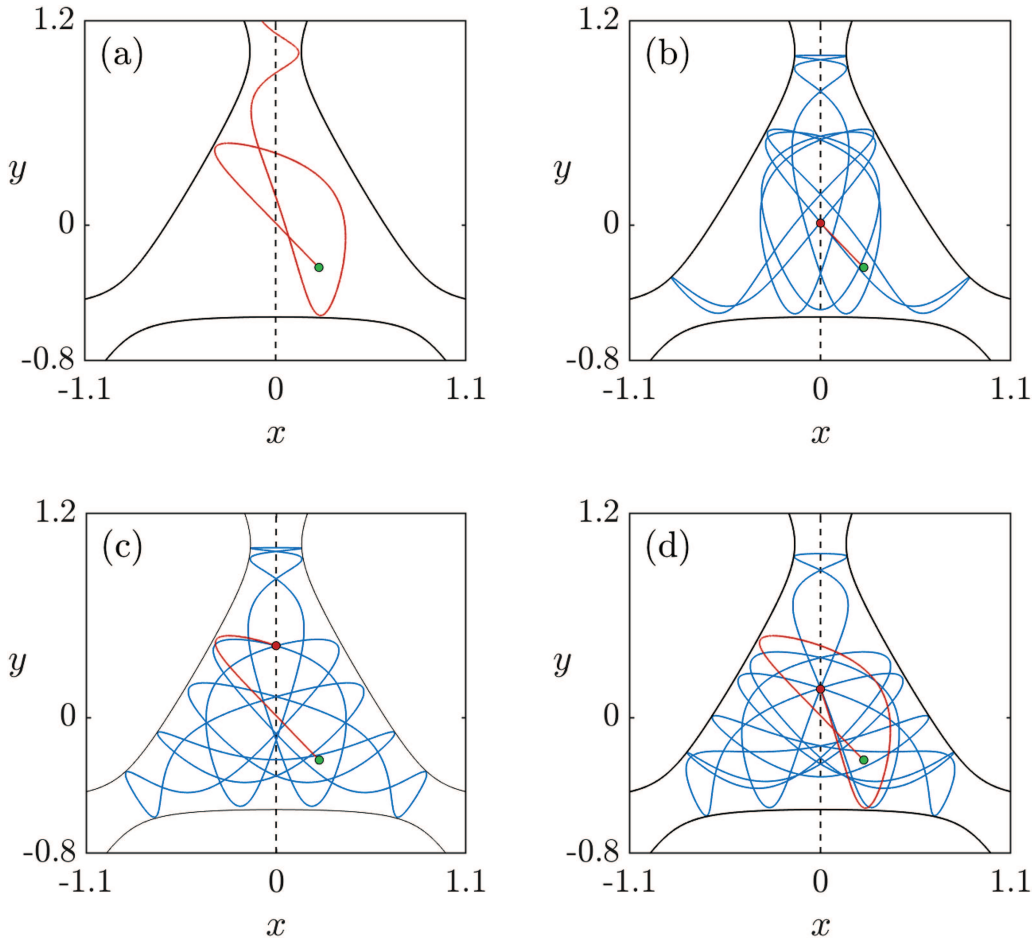

FIG. 3. Different trajectories starting from the same initial condition (see green dots in the figure). In panel (a), a trajectory without control is represented, while in panels (b), (c), and (d), a control force is activated in the first, second, and third crossing with the y axis, respectively. The color of the curves in panels (b)–(d) represents the trajectory before (red) and after (blue) the control is applied. The red dots indicate the position where the control is activated. The values of the coupling constant and the maximum required force are (b) $F = 0.054$, $K = 1.1$, (c) $F = 0.065$, $K = 1.7$, and (d) $F = 0.044$, $K = 1.6$.

momentum variables since, due to the time-reversal symmetry, if $(0, y_s, \dot{x}_s, \dot{y}_s)$ belongs to an SPO, so does $(0, y_s, -\dot{x}_s, -\dot{y}_s)$. In other words, the time direction of the SPO can be perfectly reversed in order to be closer to the trajectory that we want to control.

Once we have selected the closest crossing to our trajectory, we introduce a coupling force with the SPO associated with that crossing. With the control included, the equations of motion read

$$\begin{aligned} \dot{x} &= p_x, \\ \dot{y} &= p_y, \\ \dot{p_x} &= -x - 2xy + K(\dot{x}_s - \dot{x}), \\ \dot{p_y} &= -y - x^2 + y^2 + K(\dot{y}_s - \dot{y}), \end{aligned} \tag{4}$$

where K is a coupling constant and $\dot{x}_s, \dot{y}_s$ are the momentum coordinates of the SPO that we are trying to stabilize.

The coupling terms can be understood as a vector force with modulus $F = K\sqrt{(\dot{x}_s - \dot{x})^2 + (\dot{y}_s - \dot{y})^2}$. Therefore, the control consists of introducing continuous accelerations to direct the trajectory toward a desired periodic state. The value of F and the direction of the control force vary with time, depending on the distance between the trajectory and the target SPO. Since the majority of the SPOs with which we couple the trajectories are unstable, the control term should be continuously forcing the trajectory. Nonetheless, once the trajectory is close to the desired state, the control term is negligible and only very small corrections are necessary. The only case in which the control can be turned off is when the SPO is stable.

In a general situation, one of the limitations of the implementation of the control method might be the magnitude of the force that we can generate. For this reason, we have considered in our simulations that a maximum coupling force F_m exists, which can be introduced in the system. This means that we say that the control

has been successfully achieved if the trajectory converges to the target SPO and $\forall t, F(t) < F_m$. Otherwise, we say that the control is not possible.

Another important issue is the value of the coupling constant K. On one hand, if it is very strong, it could be counterproductive. In addition, it could generate physically meaningless strong forces. On the other hand, if the coupling is very weak, the trajectory will escape even if the control is applied. Depending on the value of K, the stabilization of the SPO will be possible or not. Even when stabilization is possible, different values of K will generate a different trajectory before the convergence to the target SPO. Therefore, the maximum required force depends on the value of K. To deal with this issue, one option is to try the stabilization with different values of K and choose the one that minimizes the maximum necessary. In all our simulations, we have tried coupling constants between 0.1 and 4 in steps of 0.1. With this procedure, we can find an optimal response of the system. However, we highlight that we have tested that the overall efficacy of the method is not significantly reduced when choosing a constant value $K = 1$.

Once we have explained the control scheme, we show its application to a particular case. The initial condition $(x_0, y_0) = (0.25, -0.25)$, launched toward $(x, y) = (0, 0)$, crosses five times the y axis before escaping in a short time $t = 12$ [see Fig. 3(a)]. Nevertheless, it is possible to avoid the escape by introducing appropriate coupling forces in any of the first three crossings. Despite this, it is not possible to avoid the escape by introducing the control in the last two crossings. The result of the three options of control is represented in panels (b), (c), and (d) of Fig. 3. The evolution of the trajectory before the control is introduced is colored in red, while the controlled orbit is represented in blue. The green dot is located in the initial condition, while the red dot represents the position where the control is activated. As we can see, the SPO that is stabilized changes depending on the crossing where we introduce the control.

To show the evolution of the control force and the energy of the system, we represent both magnitudes in Fig. 4. The data have been obtained from the numerical simulation of the previous example, concretely in the case where the control is introduced in the first crossing with the y axis. As we can see, both quantities fluctuate until reaching stabilization. The modulus of the control force is almost negligible after $t = 100$, which is the approximate value where the energy returns to the original value $E = 0.2$. We highlight that the fluctuation in the energy is very low, not exceeding 5% of the reference value.

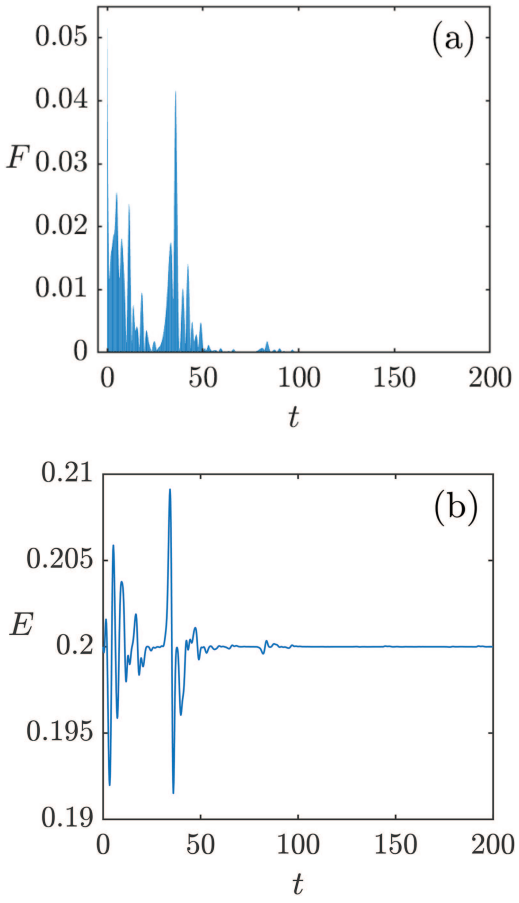

FIG. 4. Example of the typical evolution of (a) the modulus of the control force and (b) the energy of the system when the control technique is applied. The data have been obtained from the trajectory that we have represented in panel (b) of Fig. 3.

V. GENERAL EFFECTIVENESS OF THE METHOD

In this section, we test the effectiveness of the control method by trying to avoid the escape of many initial conditions distributed along all the phase space. To do so, we choose the initial conditions in two representative Poincaré sections: the (x, y) plane and the $(y, \dot{y})$ plane. Since the system has three free variables (the fourth is determined by the energy), in both cases, we have to fix one more variable or to add a constraint to the shooting. In the case of the $(y, \dot{y})$ plane, we simply define $x = 0$, and, hence, $\dot{x}$ is given by the Hamiltonian. On the other hand, in the (x, y) plane, we prefer not to fix any of the momentum but the direction of the shooting. Once the initial coordinates (x_0, y_0) are chosen, we launch the trajectory toward $(x, y) = (0, 0)$.

Once the shooting methods are defined, we divide the corresponding plane into a grid of initial conditions. For each one of them, we follow the trajectory until it escapes, recording all its crossings with the y axis. Next, in each one of the crossings, we find the closest SPO among the ones that we have previously located. At that time, we try to achieve the stabilization of the trajectory in every crossing. For this task, we try different coupling constants. Finally, we consider the crossing and the coupling constant that minimize the required force. The general results are shown in Fig. 5, where grids of 500×500 initial conditions have been used. The colors indicate the maximum required force for achieving the stabilization. Cold colors refer to low forces, while hot colors indicate high forces. For each Poincaré section, we have considered two situations where the maximum acceptable force is $F_m = 0.1$ [panels (a) and (b)] and $F_m = 0.02$ [panels (c) and (d)]. White regions inside Hill's

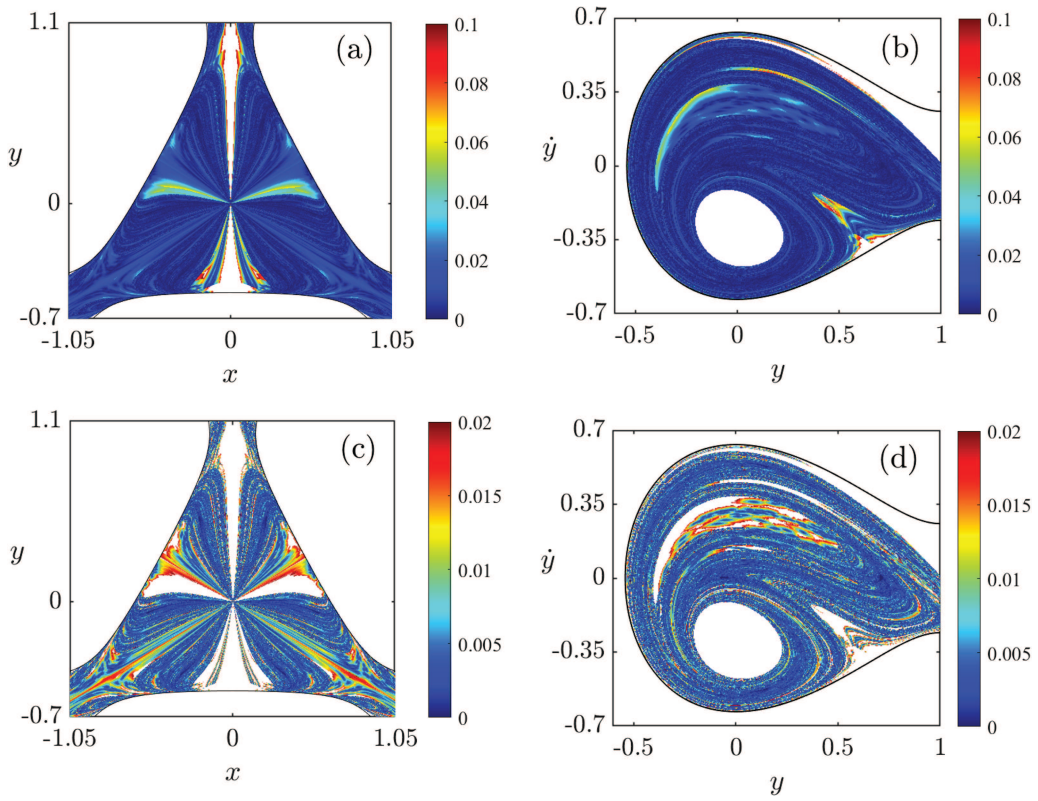

FIG. 5. Color-coded representation showing the required force to avoid the escape of many initial conditions distributed in a grid along the (x, y) plane [panels (a) and (c)] and the $(y, \dot{y})$ plane [panels (b) and (d)]. Cold colors refer to low forces, while hot colors indicate high forces. White dots inside Hill's region refer to initial conditions that cannot be controlled with the given maximum force $F_m = 0.1$ [panels (a) and (b)] and $F_m = 0.02$ [panels (c) and (d)]. The percentage of initial conditions that can be controlled depends on the maximum force and plane considered: (a) 94% (b) 86%, (c) 82%, and (d) 78%.

region (represented with dark solid lines) correspond to initial conditions that cannot be retained in the scattering region with the given maximum force.

These results confirm that it is possible to avoid the escape of a high percentage of initial conditions. In particular, by considering $F_m = 0.1$, 94% $[(x, y)$ plane] and 86% $[(y, \dot{y})$ plane] of the total initial conditions can be satisfactorily controlled. These percentages are reduced to 82% and 78% in the case of considering $F_m = 0.02$.

We highlight that the general effectiveness of the method does not vary significantly when deciding to apply the control always in the first crossing. Moreover, as we have mentioned before, we have tested that it is also possible to choose the same coupling constant for all the initial conditions ($K = 1$ is the most convenient value in this system). Of course, this goes hand in hand with assuming greater coupling forces.

Looking at Fig. 5, we can observe that there are large regions consisting of initial conditions that cannot be controlled. In fact, even if we consider clearly higher maximum forces, the percentage of controllable initial conditions cannot be significantly increased. The reason is that these regions are located far away from the stable manifold of the chaotic saddle. Therefore, their dynamics is less intertwined with the periodic orbits and they leave the scattering region in short times. Moreover, in some hopeless cases, the trajectories do not even cross the y axis before leaving the scattering region.

The regions consisting of controllable initial conditions shown in Fig. 5 resemble the stable manifold of the chaotic saddle, which has been computed in Ref. 23. Since for the control method we are using a set of periodic orbits that are embedded within the chaotic saddle, it is natural that the initial conditions that we can control are exactly the ones that are close to its stable manifold. For comparative purposes, we have computed the stable manifold of the chaotic saddle in the same Poincaré sections considered in Fig. 5. The result is shown in Fig. 6, where a good correspondence can be found between the stable manifold and the set of controllable orbits. To carry out this simulation, we have taken into consideration that in many dissipative dynamical systems with two or more different attractors, the points lying in the boundary of the basin of attraction correspond to points belonging to the stable manifold of the chaotic set.[24] Bearing this in mind, the stable manifold can be obtained simply by computing the basin boundary. In the Hamiltonian systems

studied here, exit basins[25] play the role of basins of attraction. We say that the exit basin of the exit i of an open Hamiltonian system is the set of initial conditions whose trajectories escape through the exit i. Therefore, exit basins can be computed numerically by shooting initial conditions and recording the exit through which they escape. On the other hand, the basin boundary is obtained as the set of initial conditions that have at least one nearest neighbor that escapes through a different exit.

The good correspondence between the stable manifold of the chaotic saddle and the set of controllable points implies that for every initial condition lying close to the stable manifold, we can find an arbitrarily close SPO. For simplicity, we consider only a small number of SPO, but by considering higher numbers, the required forces can be arbitrarily reduced. However, this also implies that the effectiveness of the method is directly linked to the size of the chaotic saddle. Specifically, the larger it is, the greater the percentage of initial conditions that we can control. Interestingly, the chaotic saddle is responsible for the chaotic dynamics, but it is also composed of an infinite set of periodic orbits that can be used to control the escape of trajectories. In this way, there is a counterintuitive relationship between the complexity of the phase space and the possibility of controlling the trajectories.

VI. STABILIZING THE SYSTEM IN A TARGET SYMMETRIC PERIODIC ORBIT

The previous results provided strong numerical evidence confirming that it is possible to control the escape of all the initial conditions located close to the stable manifold of the chaotic saddle. In this section, we investigate the possibility of not only avoiding the escape but also choosing the SPO that we want to stabilize.

We can imagine that we want to stabilize certain initial conditions into a concrete SPO. The reason could be that it has a particularly beneficial period or it passes through a point of interest. In general, it happens that our initial condition does not cross the y axis close to this SPO. In this scenario, the previous method leads to the stabilization of the trajectory into an SPO in which we are not interested. However, if we do so, our system will be describing a controlled periodic motion into some SPO. At this point, nothing prevents us from repeating the coupling process again and moving between different SPOs until reaching our target. This is the basic idea of the technique that we have implemented.

Every SPO crosses the y axis in multiple points, some of them being close to other SPOs. In fact, as we have mentioned in Sec. V, the periodic orbits are dense in the chaotic saddle, so we can always find a different SPO arbitrarily close. Nevertheless, the goal of our method is to control the escape with a finite number of SPOs, there will surely be some non-negligible distance between them.

The method that we have used to move between SPOs is as follows. For some initial SPO, we want to know whether it is possible or not to move to a target SPO by changing the coupling force in the appropriate time and crossing with the y axis. To do so, we have to choose in which crossing of the initial SPO we will stop the actual coupling and in which crossing of the target SPO we will introduce a new coupling. For this purpose, we calculate the Euclidean metric in the $y - \dot{y}$ plane between all the crossings of the initial and target SPO. We consider that the most favorable combination of crossings is the one that minimizes such metric. For example, if both initial and target SPO cross the y axis 8 times, we have 64 combinations of crossings where we can change the coupling from the initial to the target.

Once this is done, we calculate the optimal coupling constant and the required force. If in our numerical scheme this force is acceptable, we say that it is possible to move between these SPOs. Repeating this procedure for every single SPO, we construct a map of all the possible paths that connect the SPOs between each other. Moreover, for every initial and target SPO, we already know the

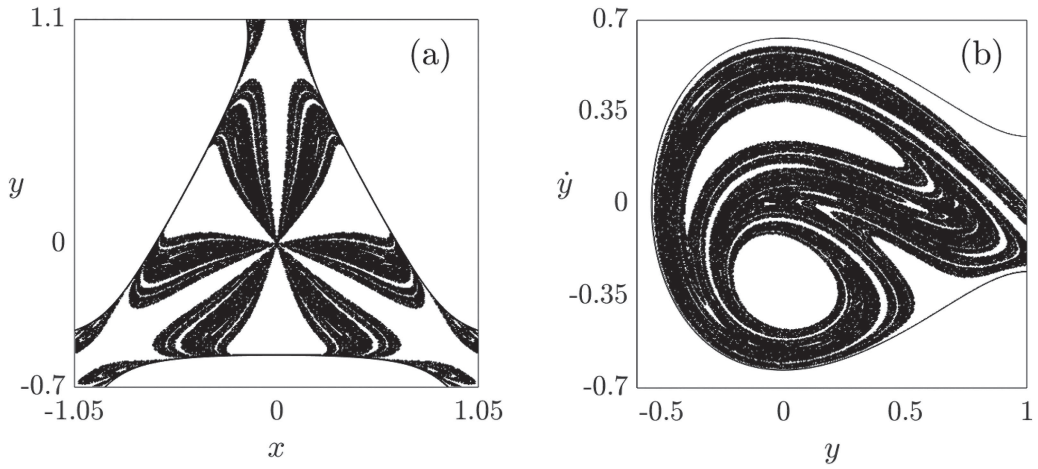

FIG. 6. Stable manifold of the chaotic saddle in the (a) (x, y) plane and (b) $(y, \dot{y})$ plane. The black dots belong to the manifold while the white ones do not. For obtaining this figure, we have computed two exit basins in different Poincaré sections and represented only the points that belong to the boundary between the basins. The resolution of each figure is 500×500. The dark solid curve defines Hill's region.

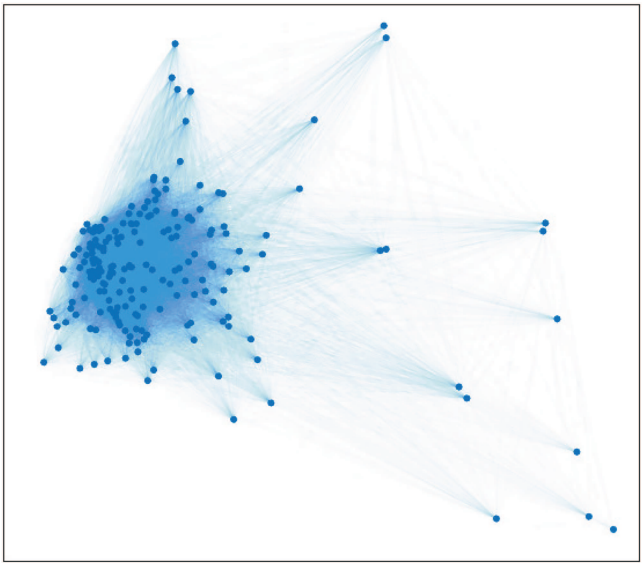

FIG. 7. Illustrative network of 200 SPOs of the Hénon–Heiles system. There is an edge between two SPOs if it is possible to move from one to the other by using a maximum control force $F_m = 0.1$.

optimal coupling constant and the required maximum coupling force. Therefore, once some initial condition is stabilized in an initial SPO, we already have the information about when and where to change the coupling terms to achieve the target SPO.

We have followed this procedure for the set of 200 SPOs that has been used in Sec. V. Surprisingly, the result shows that the network of SPOs is strongly interconnected, meaning that for a given initial SPO, there exist multiple options for moving to different SPOs. Only for illustrative purposes, we have used a graph to show the network in Fig. 7, where the nodes (dots) represent SPOs and the edges (lines) the possibility of jumping from one SPO to another with a maximum force $F_m = 0.1$.

The network represented in Fig. 7 offers a helpful visual information. However, it does not allow a deeper analysis of the method. In particular, it cannot be appreciated whether it is possible or not to connect two arbitrary SPOs. In order to bring more general information, we use a color-coded map in Fig. 8 to show the required number of jumps to move between two arbitrary SPOs. We have done the numerical simulations considering two different maximum forces $F_m = 0.1$ and $F_m = 0.02$. The colors in the grid refer to the number of necessary jumps, that can be 1 (green), 2 (blue), 3 (orange), and 4 (red). White color refers to the option of moving from one SPO to itself, so no jumps are necessary. Finally, dark colors indicate that the jump is not possible. In the higher force case [see panel (a)], most of the target SPOs can be reached after only 1 or 2 jumps, existing in only 1 connection (100 to 39) that needs 3 jumps. In the lower force case [see panel (b)], we do not observe a substantial difference. Simply, there are fewer connecting options with a single jump as well, some connections requiring three or four jumps.

In both panels of Fig. 8, a horizontal dark line can be observed, meaning that there exists one SPO that is unreachable from any other. This SPO is the Lyapunov orbit, plotted in the (a) panel of Fig. 2. Due to its special location close to the exits, it is useless in this method.

It is important to highlight that in general, the necessary force to achieve the stabilization of the initial SPO is higher than the one required to jump to a different SPO. This means that the hard part of the control method is to avoid the escape of the trajectories. Once this is done, to chose a target SPO is not challenging in terms

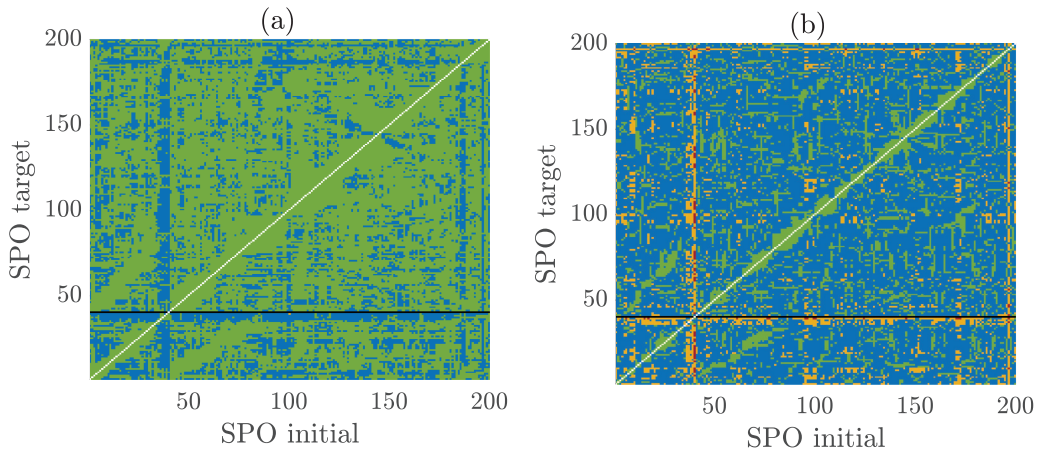

FIG. 8. A color-coded representation showing the number of jumps required to move from an initial to a target SPO. In each subplot, a different maximum force has been considered: (a) $F_m = 0.1$ and (b) $F_m = 0.02$. The colors indicate the number of required jumps, with white for zero jumps, green for one jump, blue for two jumps, orange for three jumps, and red for four jumps. The dark color indicates that the movement is not possible. This situation occurs only when trying to move from the Lyapunov orbit to any other.

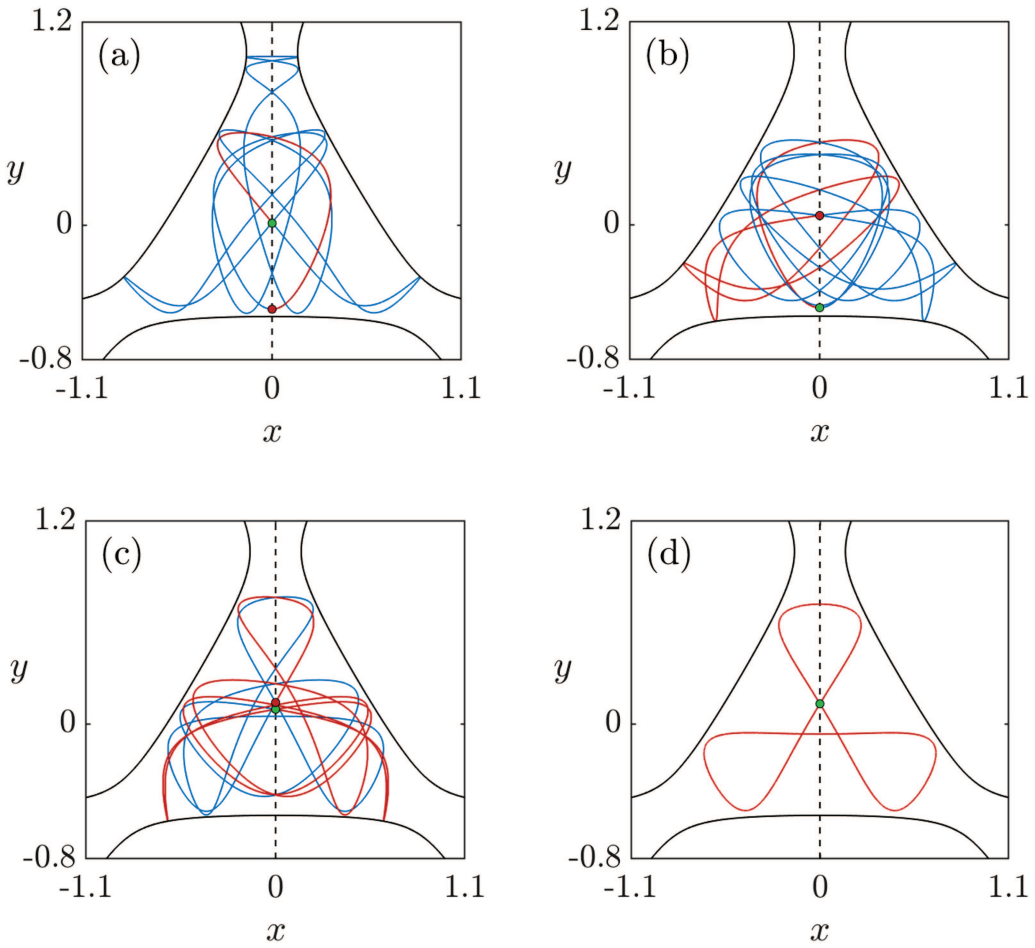

FIG. 9. In red, evolution of a single trajectory while being coupled with four different SPOs at different times. Each SPO is depicted in blue, unless in panel (d), where both the SPO and the trajectory are identical. Each panel shows only the time lapse in which the trajectory is coupled with the SPO. The green (red) dots along the y axis represent the location where the coupling with the SPO is started (finished). Then, a red dot in a panel corresponds to a green dot in the next one. If we overlap the red curves of all four panels, we obtain the whole evolution of the trajectory. All the SPOs but the one of panel (d) are unstable.

of the required coupling force. Furthermore, the intensity of the necessary force to achieve the change of SPO depends on the total number of orbits that we consider. By increasing the quantity of SPOs, and, hence, the number of crossings with the y axis, the most convenient paths between SPOs change, leading to new connections that require weaker forces. On the other hand, if we decrease significantly the number of SPOs, the connection between them is more difficult. In general, it is convenient to adapt the number of SPOs to the needs of the particular system that we want to control.

In the final part of this section, we will illustrate the previous method in a particular case. As we have mentioned in the Introduction, for an energy $E = 0.2$, the Hénon–Heiles system exhibits a unique stable SPO of low multiplicity. Naturally, it could be a convenient target because once it is reached, the control process can be finished and the trajectory will exhibit a periodic behavior forever.

Now, we consider again the same example of Sec. IV where the initial condition $(x_0, y_0) = (-0.25, 0.25)$ was launched in the direction of the origin. As we have shown, by using $F_m = 0.1$, this trajectory can be stabilized in different SPOs depending on which crossing we decide to start the control. After including the coupling force in the first crossing, the system is stabilized into a particular SPO of multiplicity $m = 8$. The maximum required force to achieve the stabilization is $F = 0.054$ (using $K = 1.1$). Here, we suppose that we want to move to the stable periodic orbit of the system. Simply knowing the initial and target SPO, the best path between them is already defined in the results of Fig. 8. By establishing $F_m = 0.02$, three jumps are required. The whole process since the trajectory is coupled with the initial SPO is represented in Fig. 9. The blue curves represent the SPO with which the trajectory is coupled, while the red curves correspond to the part of the SPO that the trajectory describes before jumping to a different one. The green dots denote the exact

location where the trajectory is coupled with the initial SPO, while the red dots represent the location where the coupling with the actual SPO finishes. The maximum required force in the first, second, and third jump is $F = 0.018$ ($K = 1.0$), $F = 0.015$ ($K = 0.5$), and $F = 0.014$ ($K = 0.1$), respectively. As we can see, the required forces to achieve the change of SPO are significantly smaller than the one necessary for the stabilization of the initial SPO.

VII. DISCUSSION AND CONCLUSIONS

In summary, we have developed here a continuous control method for avoiding the escapes in two-degree-of-freedom Hamiltonian systems. For testing the method, we have used the Hénon–Heiles system, a paradigmatic and well-known Hamiltonian in the nonlinear dynamics and celestial mechanics communities.

The method that we have implemented is based on the well-known control method by Pyragas and consists of including a control force that couples the trajectory with an SPO of the system. In particular, once the trajectory crosses the y axis, a coupling force between the trajectory and the closest SPO is introduced. Since there are infinite periodic orbits embedded within the chaotic saddle, we find the closest one from a reduced number of SPOs that have been located previously. When the control force is applied, the trajectory approaches the periodic orbit, so after some time the coupling term vanishes and the system recovers its original energy. We have shown the effectiveness of the method through numerical simulations where a limited control force is considered. The results confirm that a high percentage of escaping initial conditions can be controlled by using a relatively small quantity of SPOs as coupling options. The uncontrollable initial conditions are the ones that escape in short times and are far from the stable manifold of the chaotic saddle.

In Sec. VI, we have extended the previous method. We have shown that once the initial trajectory is stabilized into a periodic orbit, it is possible to suitably modify the coupled SPO in order to achieve jumps between different periodic orbits. The goal of this is to stabilize the system in a concrete periodic behavior in which we could be interested. We have illustrated this by stabilizing an escaping trajectory into the main stable periodic orbit of the system. Moreover, a general portrait of the possible connections between the SPOs has shown that with using a relatively small set of period orbits, it is possible to move between two arbitrary SPOs. The required coupling forces are weak and the necessary jumps are less than 4.

We hope that this work could contribute, by providing new numerical techniques, to the topic of continuous control in chaotic scattering problems. Since open Hamiltonian systems appear as a model in many different problems, we expect potential applications in various fields of science. In particular, the control scheme could be useful in restricted cases of the three-body problem[26,27] where the role of the massless body could be played by an artificial satellite subject to control. On the other hand, it could be applied to control chemical reactions in reactive systems with open channels.[28] Nevertheless, the control scheme must be adapted according to each particular problem.

ACKNOWLEDGMENTS

We acknowledge inspiring discussions with Dr. George Datseris (Max Planck Institute for Meteorology, Hamburg). The work of A.R.N., J.M.S., and M.A.F.S. has been financially supported by the Spanish State Research Agency (AEI) and the European Regional Development Fund (ERDF) under Project No. PID2019-105554GB-I00.

AUTHOR DECLARATIONS

Conflict of Interest

The authors have no conflicts to disclose.

DATA AVAILABILITY

The data that support the findings of this study are available from the corresponding author upon reasonable request.

REFERENCES

[1] Y.-C. Lai and T. Tél, *Transient Chaos: Complex Dynamics on Finite-Time Scales*, Applied Mathematical Sciences Vol. 173 (Springer, 2011).
[2] H.-J. Stöckmann, *Quantum Chaos: An Introduction* (Cambridge University Press, 1999).
[3] S. Bleher, C. Grebogi, E. Ott, and R. Brown, "Fractal boundaries for exit in Hamiltonian dynamics," Phys. Rev. A **38**, 930–938 (1988).
[4] J. M. Seoane and M. A. F. Sanjuán, "New developments in classical chaotic scattering," Rep. Prog. Phys. **76**, 016001 (2013).
[5] E. Ott, C. Grebogi, and J. A. Yorke, "Controlling chaos," Phys. Rev. Lett. **64**, 1196–1199 (1990).
[6] Y.-C. Lai and T. Tél, "Stabilizing chaotic-scattering trajectories using control," Phys. Rev. E **48**, 709–717 (1993).
[7] Y.-C. Lai and C. Grebogi, "Converting transient chaos into sustained chaos by feedback control," Phys. Rev. E **49**, 1094–1098 (1994).
[8] J. Sabuco, M. A. F. Sanjuán, and J. A. Yorke, "Dynamics of partial control," Chaos **22**, 047507 (2012).
[9] C. Chandre, M. Vittot, Y. Elskens, G. Ciraolo, and M. Pettini, "Controlling chaos in area-preserving maps," Physica D **208**, 131–146 (2005).
[10] J. H. E. Cartwright, M. O. Magnasco, and O. Piro, "Bailout embeddings, targeting of invariant tori, and the control of Hamiltonian chaos," Phys. Rev. E **65**, 045203(R) (2002).
[11] Z. Wu, Z. Zhu, and C. Zhang, "Controlling Hamiltonian chaos by medium perturbation in periodically driven systems," Phys. Rev. E **57**, 366–371 (1998).
[12] G. Ciraolo, F. Briolle, C. Chandre, E. Floriani, R. Lima, M. Vittot, M. Pettini, C. Figarella, and P. Ghendrih, "Control of Hamiltonian chaos as a possible tool to control anomalous transport in fusion plasmas," Phys. Rev. E **69**, 056213 (2004).
[13] L. Zonghua and C. Shigang, "Control of chaos in conservative flows," Phys. Rev. E **56**, 168–171 (1997).
[14] M. Hénon and C. Heiles, "The applicability of the third integral of motion: Some numerical experiments," Astron. J. **69**, 73–79 (1964).
[15] K. Pyragas, "Continuous control of chaos by self-controlling feedback," Phys. Lett. A **170**, 421–428 (1992).
[16] R. H. G. Helleman and T. Bountis, "Periodic solutions of arbitrary period, variational methods," in *Stochastic Behaviour in Classical and Quantum Hamiltonian Systems*, edited by G. Casati and J. Ford (Springer, 1979), Vol. 93.
[17] J. D. Hadjidemetriou, "Periodic orbits in gravitational systems," in *Chaotic Worlds: From Order to Disorder in Gravitational N-Body Dynamical Systems*, edited by B. A. Steves, A. J. Maciejewski, and M. Hendry (Springer, 2006).
[18] R. Barrio and F. Blesa, "Systematic search of symmetric periodic orbits in 2DOF Hamiltonian systems," Chaos Solition. Fract. **41**, 560–582 (2009).
[19] R. C. Churchill, G. Pecelli, and D. L. Rod, "Stability transitions for periodic orbits in Hamiltonian systems," Arch. Ration. Mech. Anal. **73**, 313–347 (1980).

[20]G. Contopoulos, "Asymptotic curves and escapes in Hamiltonian systems," Astron. Astrophys. **231**, 41–55 (1990).
[21]J. D. Hadjidemetriou, "The stability of periodic orbits in the three-body problem," Celestial Mech. **12**, 255–276 (1975).
[22]C. Skokos, "On the stability of periodic orbits of high dimensional autonomous Hamiltonian systems," Physica D **159**, 155–179 (2001).
[23]J. Aguirre, J. C. Vallejo, and M. A. F. Sanjuán, "Wada basins and chaotic invariant sets in the Hénon-Heiles system," Phys. Rev. E **64**, 066208 (2001).
[24]H. E. Nusse and J. A. Yorke, "Wada basin boundaries and basin cells," Physica D **90**, 242–261 (1996).
[25]G. Contopoulos, *Order and Chaos in Dynamical Astronomy* (Springer, Berlin, 2002).
[26]E. E. Zotos, H. Albalawi, T. C. Hinse, K. E. Papadakis, and J. L. Alvarellos, "Quantitative orbit classification of the planar restricted three-body problem with application to the motion of a satellite around Jupiter," Chaos Solition. Fract. **152**, 111444 (2021).
[27]A. Celletti and V. Sidorenko, "Some properties of the dumbbell satellite attitude dynamics," Celestial Mech. Dyn. Astron. **101**, 105–126 (2008).
[28]S. Kawai, A. D. Bandrauk, C. Jaffé, T. Bartsch, J. Palacián, and T. Uzer, "Transition state theory for laser-driven reactions," J. Chem. Phys. **126**, 164306 (2007).